Journal of Catalysis **200,** 270–287 (2001)
doi:10.1006/jcat.2001.3215, available online at http://www.idealibrary.com on IDEAL®

$NO + CO + O_2$ Reaction Kinetics on Rh(111): A Molecular Beam Study

Chinnakonda S. Gopinath[1] and Francisco Zaera[2]

Department of Chemistry, University of California, Riverside, California 92521

Received September 28, 2000; revised February 19, 2001; accepted February 23, 2001; published online May 15, 2001

Steady-state rates for the chemical conversion of $NO + CO + O_2$ mixtures on Rh(111) surfaces have been measured by using a molecular beam setup with mass spectrometry detection. The changes in the partial pressure of reactants (NO, CO, O_2) and products (N_2 and CO_2) have been used as a measure of the reaction rates for temperatures between 435 and 766 K and varying beam compositions around those observed in automobile exhausts. The addition of oxygen was found to inhibit the activity of the rhodium catalyst toward NO reduction in most cases, as expected. The reason for this behavior, however, was determined not to be the consumption of some of the CO in the mixture by the added O_2, but rather a poisoning of the adsorption of CO by adsorbed atomic oxygen. In fact, oxygen addition to the $NO + CO$ mixtures reduces not only the rates of N_2 production, but also those of CO_2 formation. Moreover, NO was proven to always compete favorably against O_2 for the consumption of CO. Optimum reaction rates for the production of both N_2 and CO_2 are reached at temperatures around 500–600 K and under conditions leading to stoichiometric coverages of all reactants. An interesting consequence of this is the fact that with CO-rich mixtures the addition of oxygen sometimes actually facilitates, not poisons, NO reduction, presumably because it helps in the removal of the excess CO from the surface. A synergy was observed in terms of reaction rate maxima between temperature and beam composition, CO-richer mixtures requiring higher temperatures to reach comparable reaction rates. This is explained by a decrease in CO surface coverage because of the increase in desorption rate with temperature, a trend that also explains the gradual increase in poisoning of the NO reduction activity of Rh by molecular oxygen with increasing temperature. Studies on the reaction between CO and O_2 were also carried out in order to isolate and identify the contributions of the surface oxygen deposited by dissociation of molecular oxygen and by NO to the production of CO_2, and alternations between oxygen-rich and oxygen-lean beams were used to test cyclic processes as a way to better manage NO reduction under net oxidizing atmospheres.

Key Words: **NO reduction; rhodium single crystal; molecular beam; catalytic reaction kinetics; oxidizing environment.**

1. INTRODUCTION

The reduction of NO_x in gas exhaust emissions from automobiles and stationary sources is one of the key environmental problems of our century (1, 2). This has traditionally been accomplished by using the so-called three-way catalyst, a combination of Pt, Pd, and Rh particles on high-surface-area supports such as alumina (3–5). In these, the presence of rhodium in particular is indispensable because of its efficiency in reducing nitrogen oxides (6, 7). A better understanding of the unique ability of Rh to promote such reactions should help in the search for cheaper alternatives. Lately, attention has been shifted toward promoting NO reduction under fuel-lean (net-oxidizing) settings, as future generations of fuel-economy and/or diesel-based automobiles are likely to operate under those more efficient conditions. Although there are already a number of reports available on this subject (8–10), development of the basic knowledge needed to design better commercial catalysts from first principles still requires significant additional work. In a continuing study in our laboratory to characterize the detailed kinetics and mechanism of NO reduction (11–17), here we report the kinetics of that reaction under oxidizing conditions on Rh(111) single crystals.

The reduction of NO on rhodium surfaces has already been the subject of extensive studies by the surface science community (18–53). Temperature-programmed desorption (TPD) (25), X-ray photoelectron spectroscopy (22), secondary ion mass spectrometry (SIMS) (22, 42), and vibrational spectroscopy (HREELS) (24, 28) have all been used to show that NO dissociation occurs at quite low temperatures, below 300 K at low coverages, ruling out that step as rate-limiting for N_2 production. Beyond this, however, the remaining aspects of the NO reduction mechanism are still the source of some debate. For instance, it is not clear how molecular nitrogen is actually produced on the surface. It has been traditionally assumed that after NO dissociation, the resulting nitrogen surface atoms diffuse and recombine to yield N_2 (31). The alternative idea of a recombinatory step between atomic nitrogen and adsorbed NO to form an N_2O-like intermediate was initially rejected by a series of elegant isotope-labeling temperature programmed

[1] Permanent address: Catalysis Division, National Chemical Laboratory, Pune 411008, India.

[2] To whom correspondence should be addressed.

0021-9517/01 $35.00

desorption (TPD) experiments with coadsorbed NO and nitrogen (32). However, some more recent isothermal work in our laboratory strongly argues in favor of that mechanism in actual NO reducing catalytic processes (15). Also, the issue of the factors that determine the selectivity between N_2 and N_2O production has not been resolved. That selectivity appears to depend in a complex fashion on the relative coverages of all the surface species involved (36).

A significant number of papers has also been aimed at elucidating the role of the reducing agents (53–55), CO in particular (27, 29, 30, 34, 40, 41, 56, 57), on the overall catalytic conversion of NO to molecular nitrogen. The most prevalent hypothesis is that the role of the reducing agent is to facilitate the rapid removal of the surface oxygen atoms by-product of NO dissociation. However, none of the hypothesis put forward so far has been able to account for all the experimental observations, and a better kinetic description of this system is still very much in demand. In addition, the NO reduction scenario is expected to change under fuel-economy conditions, where there is less emission of reducing agents and more oxygen in the exhaust gas. For instance, it has been suggested that the extent of NO dissociation decreases on oxygen-covered Rh surfaces compared to the clean metal (25, 29), but no direct evidence of this is available to date.

In order to address the kinetic issues still unanswered in connection with the NO + CO reaction on rhodium, we have recently carried out isothermal kinetic experiments with molecular beams on Rh(111) single-crystal surfaces between 350 and 1000 K and NO : CO ratios between 4 and 0.01 (12–17). A maximum in the steady-state rate of this reaction was observed between 450 and 900 K depending on the NO : CO beam ratio (12). A synergy was seen in this system, where the loss in reactivity induced by increasing the CO concentration in the beam is partly compensated by a higher surface temperature. The role of adsorbed nitrogen atoms during the catalytic conversion of NO on Rh(111) was also probed (13). Our study clearly identified two types of kinetically different nitrogen atoms on the surface. On one hand, a critical coverage of what we denoted strongly bonded nitrogen is required in order to sustain the catalytic production of N_2. This threshold coverage can be quite large, up to half a monolayer, at low temperatures, but decreases abruptly with increasing reaction temperature. In addition, an additional small amount of more labile nitrogen was determined to be present on the surface during catalysis but to desorb rapidly after the removal of the gas-phase reactants. The latter was determined to be the one responsible for the production of molecular N_2, since the NO + CO conversion rate is directly proportional to its coverage. A direct correlation was identified between the rates in the steady-state regime and the transient when starting with a clean surface (14). Finally, isotope switching experiments provided evidence for the formation of atomic nitrogen surface islands (13). A model was proposed where the reactivity of the nitrogen atoms is determined by the local spatial distribution of those adsorbates, the atoms on the perimeter of the islands being the ones more readily available. N_2 formation was inferred to take place via a reaction with fresh NO molecules adsorbing from the gas phase to form a N–NO-type intermediate (15, 58).

In the present paper, we report results on the kinetic details of the conversion of NO + CO + O_2 mixtures between 435 and 766 K for both fuel-rich and fuel-lean beam compositions. Our study suggests that (1) the maxima in NO decomposition and nitrogen production rates are reached under conditions leading to stoichiometric surface coverages of the reactants; (2) poisoning of the NO reduction reaction by oxygen addition is accompanied by a reduction in CO_2 production, and it is not due to a competition between the two reaction; (3) instead, the inhibiting role of oxygen is to block adsorption sites for NO and CO; (4) oxygen can have a beneficial role in the NO reduction process with CO-rich mixtures, because it can help in the removal of excess adsorbed CO from the surface; and (5) NO reduction may be managed effectively by alternating the composition of the reaction mixture between oxygen-rich and oxygen-poor conditions for short intervals of time, by taking advantage of the associated transient kinetics.

2. EXPERIMENTAL

All the experiments reported here were performed in a 6.0-L stainless-steel ultrahigh-vacuum chamber evacuated with a 170 L/s turbomolecular pump to a base pressure of about 2×10^{-10} Torr. This system is equipped with a UTI 100C quadrupole mass spectrometer, a sputtering ion gun, and a molecular beam doser. A detailed description of the doser setup and of its calibration has been given elsewhere (12, 59, 60). Briefly, the doser, a 1.2-cm-diameter array of parallel microcapillary glass tubes (10 μm in diameter and 2 mm in length), aimed directly at the surface, is connected to a calibrated volume via a leak valve and a second shut-off valve which isolates it from the main vacuum vessel. The beam flux is set by filling the backing volume to a specific pressure, as measured by an MKS baratron gauge, and by adjusting the leak valve to a predetermined set point. A total flux of 1 monolayer per second (ML/s) was used in the steady-state experiment reported here unless otherwise specified. A movable stainless-steel flag is placed between the surface and the doser in order to intercept the beam at will. The contribution from the background to the measurements of the reaction rates was deemed to be less than 10% of that from the direct beam by independent calibration experiments (12, 59), and was removed from our calculations of the steady-state rates by intercepting the gas beam at given intervals and by measuring only the changes seen between the turning on and off of the beam.

A five-way valve was also fitted to the gas handling system in order to carry out fast beam switching experiments. The common port of the valve is used to connect the doser to either one of two gas reservoirs or the roughing pump, which are attached to the other four ports. Those four ports are set in a rectangular pattern; only one port can be connected to the beam at any time. In order to minimize any cross-port flow during beam switching, two of the opposite ports were connected to the roughing pump and the other two to the two independent gas reservoirs containing the two different gas mixtures. In experiments with one single beam composition, only one of the reservoirs was connected to the beam until the end of the experiment, at which point the valve was switched to the pump by 90° rotation of the main handle. In experiments where the gas composition of the beam needed to be changed rapidly, the valve was flipped twice (two 90° turns) within a second, first to one of the pumping positions, and then to the second gas reservoir.

The solid sample, an approximately rectangular (1.10×0.56 cm^2) Rh(111) single crystal, was cleaned *in situ*, initially by Ar^+ ion sputtering, and before each experiment by cycles of oxygen exposures (1×10^{-7} Torr at 900 K for up to 20 min) and annealing to 1200 K, until the NO TPD spectra reported in the literature could be reproduced (25, 42). The crystal, which could be heated resistively and/or cooled by using a liquid nitrogen reservoir to any temperature between 90 and 1200 K, was placed at a distance of 0.5 cm from the front of the doser to assure a reasonably flat gas flux profile (59, 61). The surface temperature was monitored continuously by a chromel–alumel thermocouple spot-welded to the back of the crystal, and kept constant during the kinetic runs with a homemade precision temperature controller. TPD spectra were recorded at a constant heating rate of 10 K/s. Isotopically labelled ^{15}NO (CIL, 98% ^{15}N purity), regular CO (Matheson, 99.9% purity), and oxygen (Matheson, 99.9%) were all used as supplied. The pressures of the gases in the vacuum chamber were measured with a nude ion gauge, and were calibrated for differences in ionization sensitivities (62).

The time evolution of the partial pressures of up to 10 different species, including N_2O and NO_2, was followed simultaneously in our kinetic runs by using the computer-controlled quadrupole mass spectrometer, which was placed out of the line of sight of both the beam and the crystal in order to avoid any artifacts due to possible angular profiles in either the scattered or the desorbing gases. The mass spectrometer signals for nitric oxide, nitrogen, oxygen, carbon monoxide, and carbon dioxide were calibrated independently, as described elsewhere (12, 13). Since only ^{15}N-labelled nitric oxide was used in this work, we will refer to ^{15}NO, $^{15}N_2$, and ^{15}N simply as NO, N_2, and N, respectively, hereafter. $NO:CO:O_2$ beam compositions are represented as $x:y:z$ ratios in the following text unless otherwise specified.

3. RESULTS

3.1. General Considerations

Kinetic runs were carried out for the $NO + CO + O_2$/Rh(111) system in a manner similar to that reported in our previous publications (11–17, 59, 60, 63–65). As an example of the results obtained with this approach, Fig. 1 shows raw kinetic data for the evolution of the partial pressures of ^{15}NO, CO, O_2, $^{15}N_2$, and CO_2 over time for the case of a $^{15}NO:CO:O_2$ molecular beam of 1:7:2 composition as the reaction temperature was varied between 435 and 765 K. The sequence of events in these experiments is as follows. First, the temperature of the substrate is set at 435 K. Then, molecular beam is turned on (at time $t = 2$ s) while keeping the flag in the intercepting position so the crystal is not yet exposed directly to the gas stream. Because of the scattering of the molecules from the flag into the vacuum chamber, this leads to increases in the respective partial pressures of the reactants (CO, O_2, and ^{15}NO) to new steady-state values. Notice that the partial pressure of CO_2 does increase somewhat at this point too because

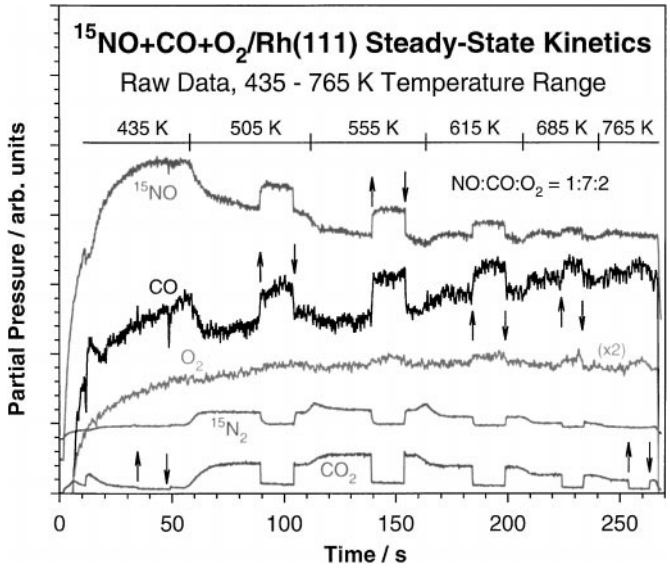

FIG. 1. Typical raw kinetic data of the type described in this report. An effusive collimated $^{15}NO + CO + O_2$ molecular beam (of 1:7:2 $^{15}NO:CO:O_2$ composition in this example) is directed onto a clean rhodium(111) surface as the temperature is swept in steps between 435 and 765 K and the partial pressures of both reactants (^{15}NO, CO, and O_2) and products ($^{15}N_2$ and CO_2) are followed as a function of time. The beam is occasionally blocked and unblocked in order to measure the steady-state rates due to the gases in the beam directly, as they are proportional to the drop in partial pressure of the products and/or the rise in partial pressure of the reactants from their steady-state values. Note the following: (1) the instantaneous changes in CO_2 signal with blocking and unblocking of the beam, in contrast with the slower response of the N_2 trace; (2) the additional N_2 desorption seen when the temperature is raised from 505 to 555 K and from 555 to 615 K; and (3) the different behavior of the O_2 uptake curve, which shows significant changes only at high temperatures.

of the conversion of the background gases. Next, the flag is removed from the path of the beam (at approximately $t = 12$ s) in order to allow for its direct impingement on the surface. This causes a transient where both decreases in the partial pressures of the reactants and increases in the signals of the products are seen before all pressures reach the new steady-state levels corresponding to the catalytic process. Notice in particular that while a jump in the CO_2 signal is seen immediately after the unblocking of the beam, the signal for the formation of N_2 rises (slightly) only after a delay of about 5 s from that point. Some CO desorption is also seen near the flag-removal point due to displacement of some adsorbed CO by the incoming NO, a phenomenon already reported for $NO + CO$ mixtures (14).

The system is allowed to evolve until a steady state is reached, which generally happens within less than 30 s of the unblocking of the beam under the experimental conditions employed here. At that point, all the signals level off except for that of NO, which continues to rise because of the poor pumping speed of the vacuum apparatus for this molecule; this latter effect does not represent any chemical change in the system, and does not affect our rate measurements. Once the steady state has been established at a given temperature, the rate is measured by blocking the beam for a few seconds and then unblocking it again to restore the original steady-state level. For example, during the steady-state regime at 435 K (the initial temperature) the molecular beam was blocked deliberately by raising the flag at $t = 35$ s, and unblocked again at $t = 49$ s. Typically, there are detectable increases in the partial pressures of the reactants and accompanying drops in the partial pressures of the products during the period where the beam is blocked; those were used here to calculate the steady-state rates of the reaction at that temperature (12–14, 59). After the rate measurements for a given temperature have been made, the crystal is quickly heated (within a few seconds) to the next temperature, and the system is allowed to stabilize again before measuring the new steady-state rate. This procedure is repeated for several temperatures, up to 765 K in this example. Finally, the molecular beam is turned off, at about $t = 265$ s in Fig. 1.

An important observation from the experimental sequence depicted in Fig. 1 is the difference in behavior of the NO, CO, and oxygen traces in terms of the extent of the adsorption of those gases at the different temperatures. For instance, at 555 K, where the CO_2 rate maximum is observed in this example, the rate of NO adsorption also reaches a maximum, but that of oxygen adsorption is still quite small. As the reaction temperature is increased, however, both the steady-state rates and the extent of the adsorption of NO and CO decrease, but an increase in oxygen adsorption is clearly seen instead. No detectable NO adsorption or nitrogen production is observed by 765 K, yet oxygen and CO are still consumed and CO_2 is still produced at that temperature. Another interesting observation to be noted is the transient increase in nitrogen partial pressure at the points where the temperature is raised from 505 to 555 K and from 555 to 615 K. This is a consequence of the desorption of the strongly bonded nitrogen coverage (Θ_N) that builds up and remains on the surface under steady state at the lower temperatures (12, 13). Finally, no signal for $^{15}N_2O$ (46 amu) was ever observed during any of the kinetic runs reported in this paper.

The possibility of any hysteresis in the behavior of the $NO + CO + O_2$ conversion on Rh(111) was tested by ramping the temperature of the surface in both up and down directions. Figure 2 displays the changes in rates seen for a beam of $1:7:2$ $NO:CO:O_2$ composition and $F_{total} = 0.25$ ML/s as a function of temperature. Three consecutive sequences are shown in this figure, namely (1) a forward ramping from low to high temperatures starting with the clean metal; (2) the accompanying reverse sequence from high to low temperature; and (3) a third ramp from low to high temperatures performed immediately afterward. The rates of nitrogen production display a total reversible behavior: identical values were measured at any given temperature in all three sequences. The rates of CO_2 production, on the other hand, do display some noticeable variations. Specifically, higher CO_2 desorption rates were measured when starting with a clean metal, even though no differences were seen in the kinetics of the $NO + CO + O_2$ conversion with temperature once the surface was exposed to the reactants at high temperatures regardless of whether the measurements were carried out under heating or cooling conditions. The results reported in the remaining of the paper were obtained by starting with the clean metal and ramping toward higher temperatures. A few kinetic measurements were made by starting with the clean metal at different high temperatures and subsequently cooling to low temperatures. In that case, the temperature at which the rate of N_2 production reaches its maximum shifts from 555 to 505 K, while that for CO_2 formation peaks at the same temperature. Clearly, some differences in reaction rates are seen depending on the history of the catalyst. This fact will be addressed in the Discussion section.

Systematic studies to measure steady-state rates for the $NO + CO + O_2$ reaction on Rh(111) surfaces as a function of beam composition were performed with three different sets of beam compositions, namely (a) with $1:9:z$ $NO:CO:O_2$ ratios, $z = 0$ to 10; (b) with $1:y:5$ $NO:CO:O_2$ ratios, $y = 4$ to 19; and (c) with $1:y:z$ $NO:CO:O_2$ ratios, $y = 9$ to 4 and $z = 9 - y = 0$ to 5. These composition ranges were chosen to simulate the gases encountered in real-world automotive exhaust processes under both fuel-lean and fuel-rich conditions. Additional studies with pure $CO + O_2$ mixtures were also carried out under similar conditions for comparison. In order to contrast the behavior of the $NO + CO + O_2$ mixtures with those of the $CO + O_2$ beams, the $NO + CO$ reaction was considered to be

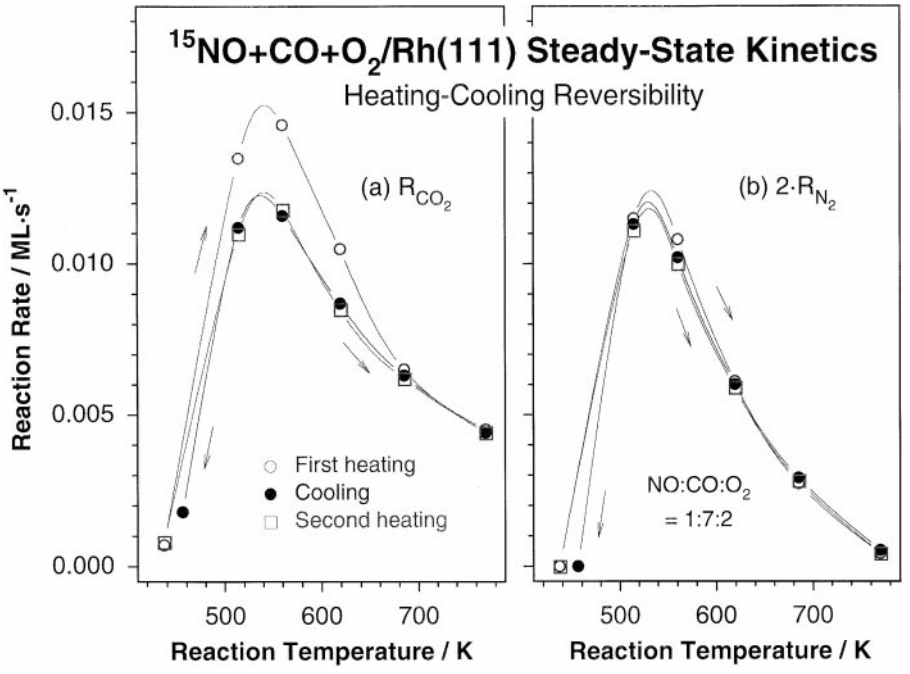

FIG. 2. CO_2 (a, left panel) and $^{15}N_2$ (b, right panel) production rates versus temperature measured for a 1 : 7 : 2 NO : CO : O_2 beam on Rh(111) as the clean surface is sequentially heated from 435 to 765 K, cooled back to 435 K, and heated a second time. The total beam flux used in this experiment was $F_{total} = 0.25$ ML/s. Note that while the same rate is observed for N_2 production at any given temperature irrespective of the history of the process, that is not true in the case of CO_2 formation, where the clean surface displays considerably higher rates at low temperatures than the contaminated substrate.

stoichiometric, so kinetic trends measured using $CO + O_2$ mixtures with $y-1:z$ CO : O_2 ratios were compared to those for $1:y:z$ NO : CO : O_2 beam compositions. The results of all these studies are summarized below.

3.2. *1 : 9 : z NO : CO : O_2 Beam Compositions, z = 0 to 10*

Figure 3 displays the time evolution of the CO_2 (left panel, a) and N_2 (right panel, b) production traces during exposure of the Rh(111) surfaces to NO : CO : O_2 beams with 1 : 9 : z compositions ($z = 0$, 1, 3, 5, 7, and 10) at crystal temperatures between 435 and 765 K. A slow conversion can be catalytically sustained even at 435 K in these cases, although there is no noticeable drop in the partial pressures of N_2 when blocking the beam at 435 K. Indeed, a little CO_2 production is observed throughout the reaction for all z values. Isothermal kinetic results from surfaces exposed to either NO or NO + CO beams under these conditions have indicated that the desorption of N_2 starts only at temperatures above 450 K (11–14), so it can be concluded that the presence of oxygen in the beam changes the threshold temperature for catalysis.

A significant increase in reactivity is seen in Fig. 3 when the crystal is heated above 505 K: there are clear changes in the partial pressures of both N_2 and CO_2 as the beam is blocked and unblocked at that temperature. It is important to note that the NO + CO + O_2 conversion rate does display a finite value even when the beam is blocked because of the conversion of background gases. However, this latter contribution amounts to only 10% or less of the rate seen with the direct beam (compare the N_2 partial pressures at 435 K with those while the beam is blocked at any other temperature to estimate the rates due to background adsorption), and can be easily subtracted by considering only the differences in rate between the points with the flag in the raised and lowered positions. Two important observations are worth mentioning in reference to the data in Fig. 3. First, the reaction rate, which is proportional to the changes in the partial pressure of the products, increases rapidly with temperature until reaching a maximum at about 555 K. Second, between 505 and 615 K, the transient kinetics for N_2 and CO_2 production are quite different. For instance, when heating from 505 to 555 K ($t = 115$ s) and from 555 to 615 K ($t = 165$ s), the N_2 desorption rate first increases abruptly, and then slowly stabilizes to its new steady-state value. As mentioned before, this is mainly due to desorption of the strongly bonded nitrogen that builds up on the surface at low temperatures.

A summary of the reaction rates obtained for the production of CO_2 (left panel, a) and of N_2 (right panel, b) with the 1 : 9 : z NO : CO : O_2 beams is shown as a function of temperature and beam composition in Figs. 4 and 5, respectively. It is seen there that the maximum reaction rates for the production of both CO_2 and N_2 are achieved around 555 K, and

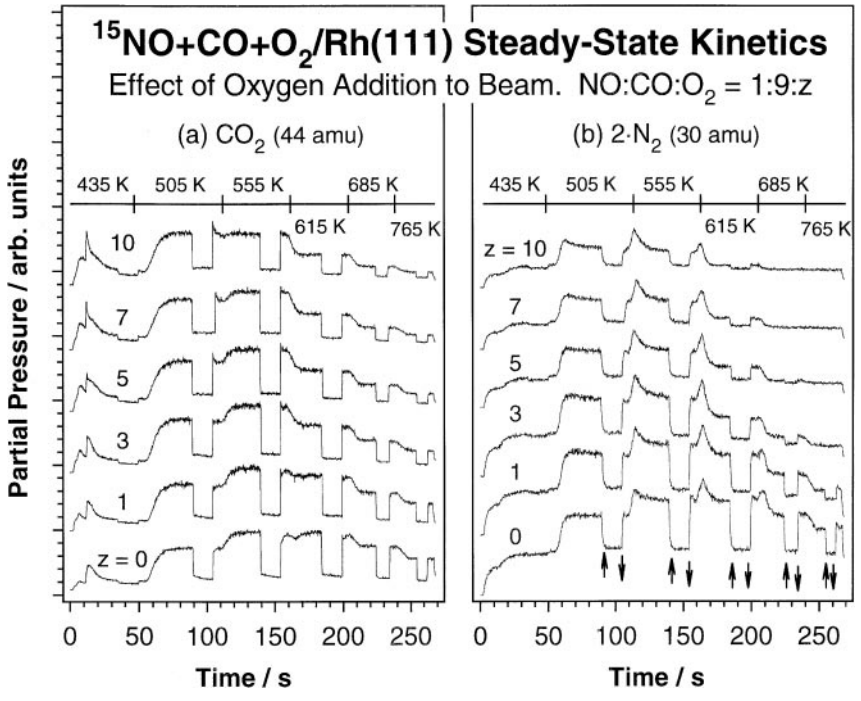

FIG. 3. Time evolution of the partial pressure of the products, CO_2 (a, left panel) and $^{15}N_2$ (b, right panel), in kinetic experiments such as that described in Fig. 1 at temperatures between 435 and 765 K. $1:9:z$ $^{15}NO:CO:O_2$ ratios were used in this set of experiments, with z varying from 0 to 10. CO_2 production is seen at all temperatures, but N_2 formation ceases at high temperatures with increasing oxygen concentration. As in Fig. 1, a slow response is seen at low temperatures in the N_2 trace upon blocking and unblocking of the beam, and desorption of additional nitrogen is seen as the temperature is raised from 435 to 615 K.

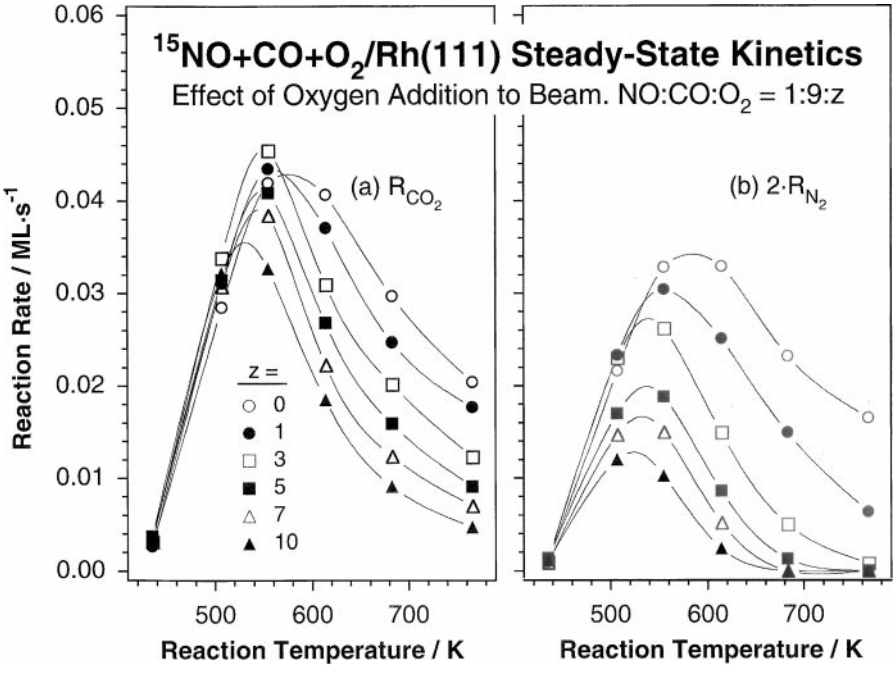

FIG. 4. Temperature dependence of the steady-state rates of formation of the products, CO_2 (a, left panel) and N_2 (b, right panel), during the conversion of NO + CO + O_2 mixtures on Rh(111) as a function of beam composition. These data were extracted from the raw partial pressure traces in Fig. 3 after appropriate calibration. Both rates increase from 435 K until reaching maxima somewhere between 555 and 615 K, after which they decrease again. The reaction rate maxima shift to lower temperatures with increasing oxygen concentration in the beam.

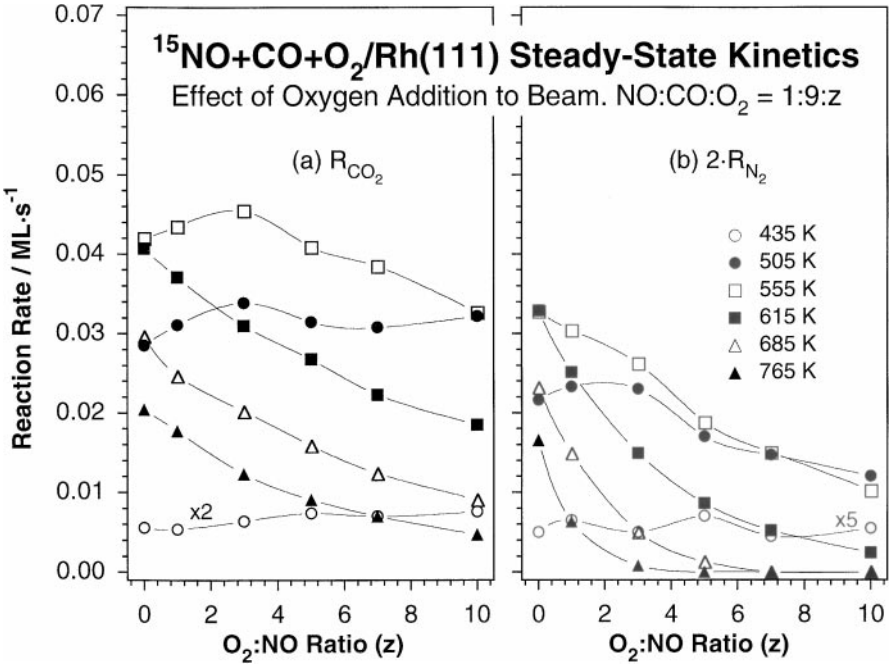

FIG. 5. Composition dependence of the steady-state rates of formation of the products, CO_2 (a, left panel) and N_2 (b, right panel), during the conversion of $NO + CO + O_2$ mixtures on Rh(111) as a function of reaction temperature. These data are the same as in Fig. 4, but are displayed as a function of O_2-to-NO ratio in the beam to highlight the competing nature of the $CO + NO$ and $CO + O_2$ reactions. Note that CO_2 production is approximately constant at 555 and 505 K regardless of oxygen content in the beam, but that it decreases with O_2 partial pressure at higher temperatures. Perhaps more interesting is the initial marginal activity increase in both CO_2 and N_2 production observed at 505 K with increasing O_2 fraction in the beam.

that those rates then decrease slowly at higher temperatures for all values of z. A number of points are to be made here: (1) as the oxygen concentration increases, the rate maxima shift slightly to lower temperatures, from 555–615 K at $z = 0$ to 505–555 K at $z = 10$; (2) the absolute rates also decrease with increasing oxygen concentration, in particular those for N_2 production; (3) the drops in CO_2 and N_2 production rates with increasing oxygen concentration are more noticeable above 550 K (at lower temperatures they remain almost constant, at least in the case of CO_2 formation); and (4) there is a clear qualitative change in behavior around $z = 3$, the effect of oxygen on reaction rates being significantly more important with higher O_2 concentrations in the beam. Note that $z = 4$ corresponds to a stoichiometric mixture in these beams.

One additional thing to point out from the data in Figs. 3 to 5 is the fact that the $N_2 : CO_2$ production ratio observed experimentally is in most cases higher than that expected from stoichiometric arguments. We attribute this difference to the competitive nature of the adsorption of NO, CO, and O_2. It would appear that NO adsorbs preferentially (compared to O_2), at least at intermediate reaction temperatures. This can be seen directly in Fig. 1 by the large changes in NO partial pressure relative to those for O_2 when the beam is blocked. Reaction rates closer to stoichiometric are seen at high temperatures and for high values of z.

3.3. *Other Beam Compositions*

The reaction rates measured for CO_2 (left panel, a) and N_2 (right panel, b) production as a function of composition (and temperature) for the $1 : y : 5$ $NO : CO : O_2$ beams are plotted as a function of $CO : O_2$ ratio in Fig. 6. The $NO : O_2$ ratio chosen here, 1 : 5, is close to that seen in automobile exhausts, so switching between fuel-lean and fuel-rich conditions could then be easily emulated by adding CO ($y = 4$ to 19) to the beam. In this set of experiments, the maximum rate of reaction shifts toward higher temperatures as more CO is added to the beam. Other points to be noted: (1) the rate maximum becomes less sensitive to temperature with increasing CO in the beam; (2) above 550 K addition of CO to the beam leads to an increase in CO_2 production rate, but at lower temperatures the rate decreases with increasing y once it reaches its maximum value; (3) a similar, although less marked, trend is seen in the production of N_2, but the rate of nitrogen production changes little when the beam is rich in CO ($y > 10$) between 505 and 615 K; and (4) at high temperatures ($T > 700$ K), the oxidation of CO by oxygen is the only reaction observed; no nitrogen is produced.

In another set of experiments, the concentrations of CO and O_2 were changed simultaneously while the absolute NO concentration was kept the same. $1 : y : z$ $NO : CO : O_2$ beam ratios with $y + z = 9 =$ constant (y, $z = 9$, 0 to 4, 5)

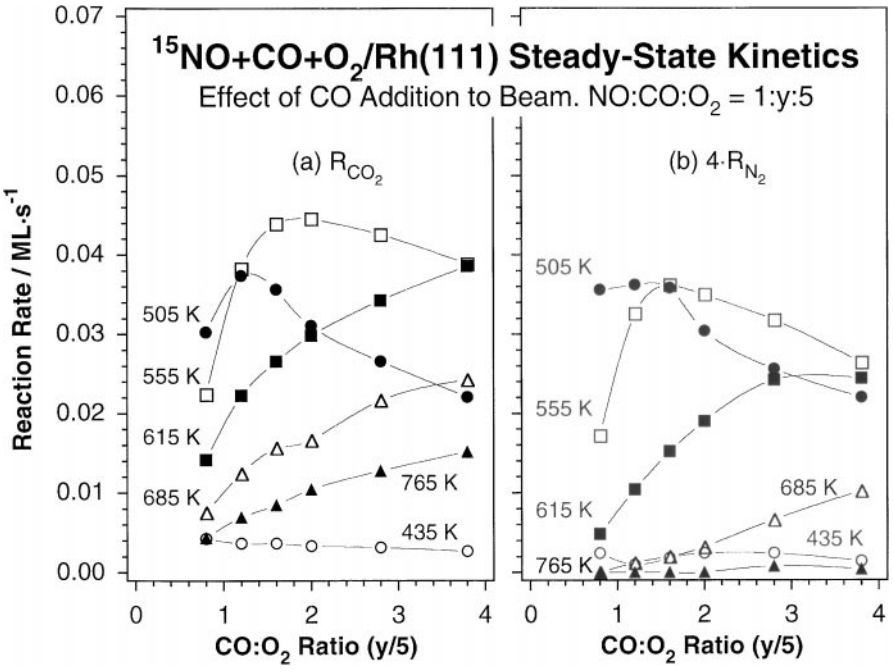

FIG. 6. Effect of the addition of CO to the activity of Rh(111) toward the conversion of NO + CO + O_2 mixtures. The dependence of the steady-state rates of formation of the products, CO_2 (a, left panel) and N_2 (b, right panel), is shown here as a function of reaction temperature for a set of beams with $1:y:5$ NO : CO : O_2 ratios, with y varying from 4 to 19. Both productions of N_2 and CO_2 are accelerated by the added CO at high temperatures, but CO poisoning is observed for high CO : O_2 ratios at low temperatures.

were employed to probe the efficiency of the NO reduction reaction while changing from net reducing to net oxidizing beam compositions. The results, shown in Fig. 7, indicate basically the same behavior reported with the previous beam sets. In addition, it is seen that (1) at high temperatures, above 600 K, oxygen-rich beams ($z/y > 1$) display a significant decrease in NO reduction capacity, with rates at least an order of magnitude lower than those measured with no oxygen; (2) in contrast, most of the NO reduction activity is retained at low temperatures; (3) a reverse in reactivity trends is seen at $T = 505$–555 K for $z/y \sim 0.5$; and (4) the maximum in CO_2 production rate is reached at 555 K with the $1:7:2$ NO : CO : O_2 beam. Notice that this corresponds to the stoichiometric composition in this set, which is somewhere between $y = 6$ and $y = 7$ ($z/y \sim 0.5$–0.3). On the other hand, N_2 production is almost always optimized by reducing the concentration of oxygen in the beam.

3.4. *Competition between O_2 and NO for CO Oxidation*

In order to estimate the relative rates for the CO + O_2 versus CO + NO reactions, rate differences between CO_2 and $2\times$ N_2 production were plotted versus temperature in Fig. 8. The positive rate difference observed for all beam composition at all temperatures clearly demonstrates an increase in the rate of oxidation of CO when O_2 is added to the beam. In the case of the $1:9:z$ beam compositions (Fig. 8a), this rate difference increases initially as the beam becomes richer in oxygen, as expected, but levels off for $z \geq 5$ at intermediate temperatures, and decreases significantly above 600 K, especially with oxygen-rich beams. It is worth pointing out that the latter changes are likely to reflect the behavior of the CO + O_2 reaction, because no N_2 is produced for $z \geq 3$ at 765 K (Fig. 4).

In the case of the $1:y:5$ beams (Fig. 8b), the maximum $CO_2 - 2\times N_2$ rate differential also occurs at 555 K, but it extends to 615 K for CO-rich ($y = 19$) beams. Moreover, this rate difference increases in an approximately linear fashion with increasing CO concentration at all temperatures except 505 K (where it in fact decreases with increasing y). Note, however, that all the beams used in this set can be considered rich in CO, in the sense that the total reduction of the NO would only require $y = 1$. The reverse trend at 505 K suggests that the surface may be poisoned there by the excess CO in the beam. Since the resident time of CO on the surface decreases with increasing temperature, this effect becomes less pronounced, hence the higher CO + O_2 reaction observed as the crystal is heated further.

When considering the $1:y:z = 9-y$ beams (Fig. 8c), $CO_2 - 2\times N_2$ rate differential maxima are again obtained at 555 K for all values of y. Also, the rate difference first increases with decreasing y, but then reverts for $y \leq 6$ (CO : $O_2 \leq 0.5$). This indicates that there is an optimum beam composition where the rate of CO oxidation by O_2 in the presence of NO is maximized.

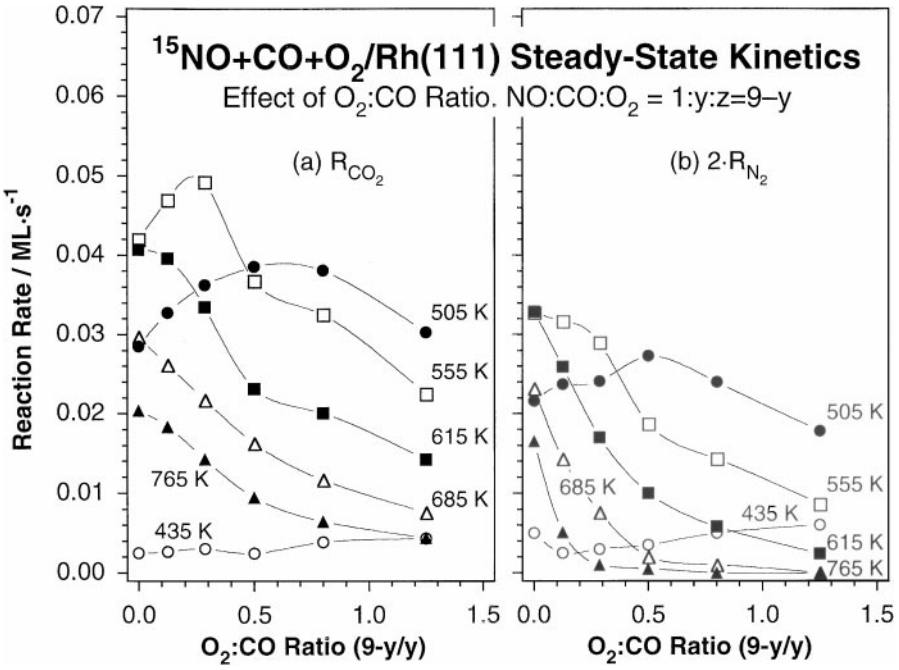

FIG. 7. Effect of the change in $CO:O_2$ ratio to the activity of Rh(111) toward the conversion of $NO + CO + O_2$ mixtures. The dependence of the steady-state rates of formation of the products, CO_2 (a, left panel) and N_2 (b, right panel), is shown here as a function of reaction temperature for a set of beams with $1:y:z = 9-y$ $NO:CO:O_2$ ratios, with y varying from 0 to 9. Optimum rates are seen under conditions leading to stoichiometric coverages on the surface. This is best observed at low temperatures, in particular by the rate maxima reached at 505 K with the $1:6:3$ $NO:CO:O_2$ beam.

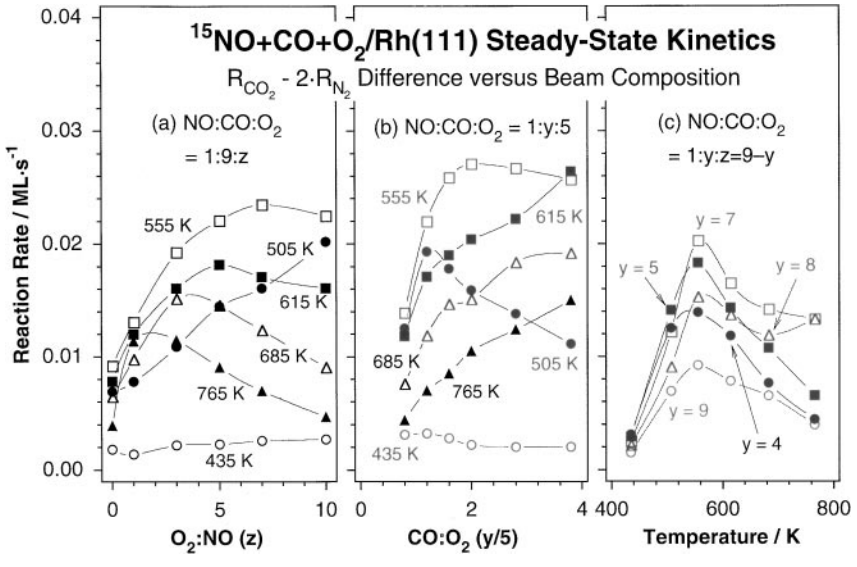

FIG. 8. Estimates of the rates of oxygen consumption during the conversion of $NO + CO + O_2$ mixtures on Rh(111) as a function of temperature and beam composition. Rate differences between CO_2 and $2 \times N_2$ production are displayed here in three panels for the three sets of beam compositions reported in the previous figures. Left (a): Rate differentials versus $O_2:NO$ ratio for the $1:9:z$ $NO:CO:O_2$ beams at different temperatures between 435 and 765 K. Center (b): Rate differentials versus $CO:O_2$ ratio for the $1:y:5$ $NO:CO:O_2$ beams at different temperatures between 435 and 765 K. Right (c): Rate differentials versus temperature for the $1:y:z = 9-y$ $NO:CO:O_2$ beams, $y = 4$ to 9. Some CO_2 production from the $CO + O_2$ reaction is seen in all cases, but never at rates comparable to those seen for the reduction of NO. Clearly, NO competes favorably against O_2 for the adsorbed CO.

3.5. CO Oxidation Kinetics by O_2

The rates of the $CO + O_2$ reaction were measured independently by using $CO + O_2$ beams with compositions equivalent to those in the $NO : CO : O_2$ beams of $1 : y : z = 9 - y$ ratios. For this, we assume that the NO + CO reaction is stoichiometric, so $y - 1 : z$ $CO : O_2$ ratios were used to account for the consumption of one molecule of CO by each molecule of NO. The results from the $CO + O_2$ experiments with different beam compositions and at different temperatures are plotted in Fig. 9. With CO-rich beams ($y - 1 : z \geq 2$) the maximum in CO_2 production rate occurs at 555 K, but that rate increases further and maximizes at lower temperatures with more oxygen in the beam. The optimum rate is seen at 505 K and $y - 1 : z = 5 : 3$; further decreases in rate are seen with additional increases in oxygen concentration at all temperatures. A synergistic effect is observed between beam composition and reaction temperature, indicating that changes in composition are at least partly compensated by changes in reaction temperature. A similar temperature–beam composition interdependence reported for the case of NO + CO on Rh(111) was explained by an optimization in the relative coverage of the reactants on the surface (12).

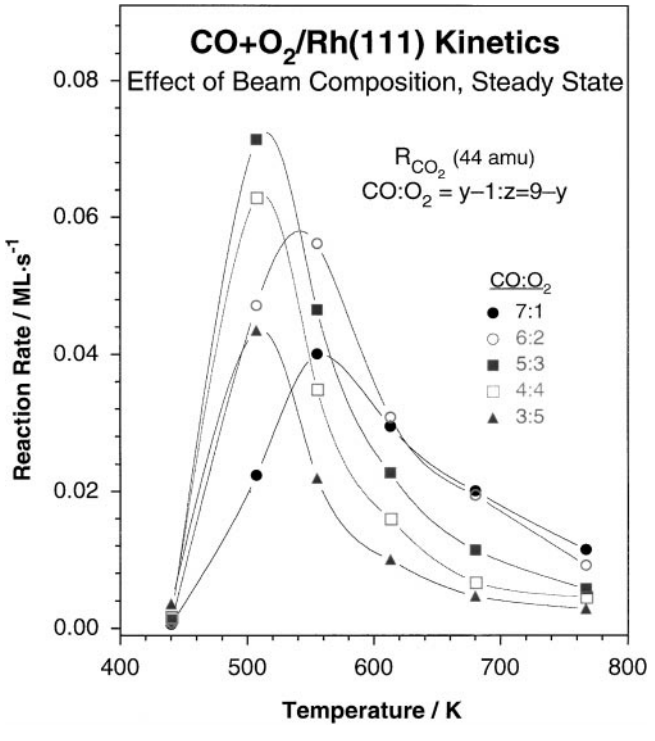

FIG. 9. Temperature dependence of the steady-state CO_2 formation rate for different $CO + O_2$ beams with $y : z = 9 - y$ $CO : O_2$ ratios, $y = 3$ to 7. As in the case of the $NO + CO + O_2$ mixtures, the rate maximum of CO_2 formation shifts from 505 to 555 K as the beam becomes richer in CO. The maxima are seen for stoichiometric surface coverages, and the fastest reaction is seen at 505 K and for a 5 : 3 $CO : O_2$ beam.

A comparison of the data in Fig. 8c and 9 allows for the quantification of the effect that NO has on the $CO + O_2$ reaction. This is best illustrated by the differences in CO_2 production rate between the experiments with the $y - 1 : z$ $CO : O_2$ and $1 : y : z$ $NO : CO : O_2$ beams, which are plotted versus temperature in Fig. 10a. The CO_2 production rate difference appears to be negative at all temperatures with the CO-richest beams ($CO : NO = 8 : 1$), but this could be due to experimental uncertainties. At the other end, the rate difference becomes the most significant at temperatures around 500 K, and peaks at $CO : O_2$ ratios close to stoichiometric ($NO : CO : O_2 = 1 : 6 : 3$).

The effect that oxygen has on the production of molecular nitrogen is explored by the data in Fig. 10b. There, the results provided in Fig. 4 for $1 : 9 : z$ $NO : CO : O_2$ mixtures are expanded to other $NO : CO$ ratios. Also, the difference in nitrogen production rate between oxygen-free and oxygen-containing beams is emphasized here. Addition of O_2 to a given NO + CO beam is expected to consume some of the carbon monoxide in the mixture, and to therefore reduce the rate of nitrogen formation, and this is indeed what is observed in most cases. There are, however, some conditions under which the addition of oxygen actually enhances the rate of N_2 production. Specifically, increases in that rate with oxygen addition are seen for temperatures between about 500 and 550 K. This effect is more pronounced in CO-rich mixtures as oxygen is added up to stoichiometric mixtures.

3.6. Beam Switching Kinetic

The experiments described so far correspond to steady-state rate measurements on the NO + CO + O_2/Rh(111) system as a function of temperature and beam composition. In describing those, the changes that occur when going from oxygen-rich to oxygen-lean beams have been highlighted. The influence that pretreatment of the sample has on the kinetics of NO reduction has also been discussed (Fig. 2). By using the five-way valve setup described in the Experimental section, the behavior of the system under oscillatory conditions could be probed directly. A number of kinetic runs were performed where the Rh surface was alternatively exposed to oxygen-rich and oxygen-lean beams. In the example presented in Fig. 11, an initial beam of $1 : 4 : 5$ $NO : CO : O_2$ ratio was alternated with a second one of $1 : 9 : 0$ composition while maintaining the surface temperature constant at 615 K. This figure displays the raw data for the partial pressures of NO, N_2, and CO as a function of time, normalized to the same total beam flux. This latter adjustment was required to compensate for the drop in backing pressure behind the doser induced by pumping of the intermediate volume common to the two gas reservoirs every time the beam was switched (this problem could be minimized by using larger gas reservoirs). It can be seen in Fig. 11 that the reaction with the oxygen-rich (1 : 4 : 5)

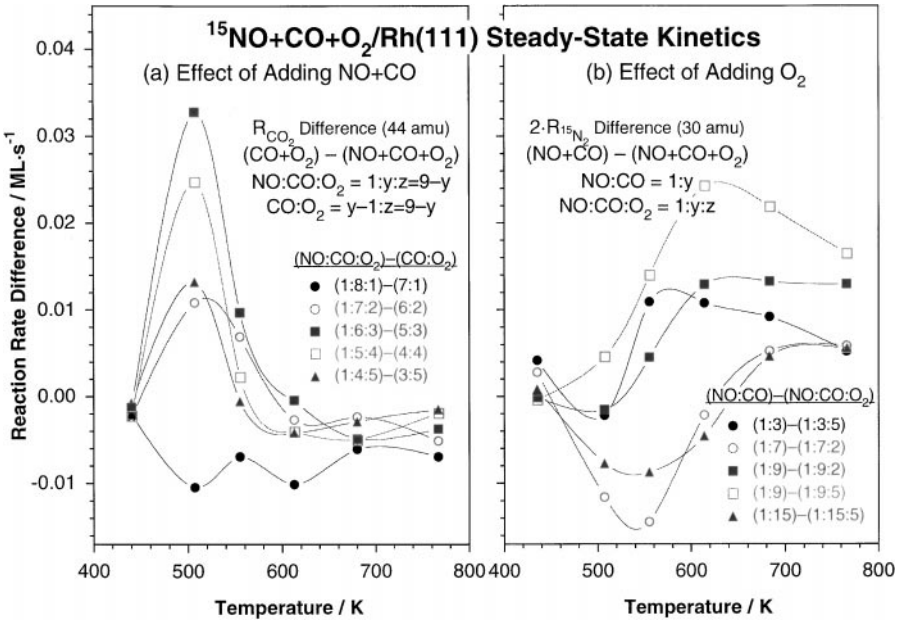

FIG. 10. Left (a): Measure of the effect of adding a 1 : 1 NO : CO mixture to the conversion of different $CO + O_2$ beams. Plotted here is the CO_2 rate difference between $y - 1 : z = 9 - y$ CO : O_2 and $1 : y : z = 9 - y$ NO : CO : O_2 beams for $y = 4$ to 8 as a function of surface temperature. Significantly higher rates are generally seen in the absence of NO in the beam, in particular below 600 K. Right (b): Measure of the effect of adding oxygen to $NO + CO$ beams of different compositions. The difference in N_2 production rate, without minus with oxygen, is plotted as a function of temperature for a number of beam compositions. Typically, O_2 poisons the NO reduction to N_2, but some rate enhancement is seen between 500 and 600 K with CO-rich beams.

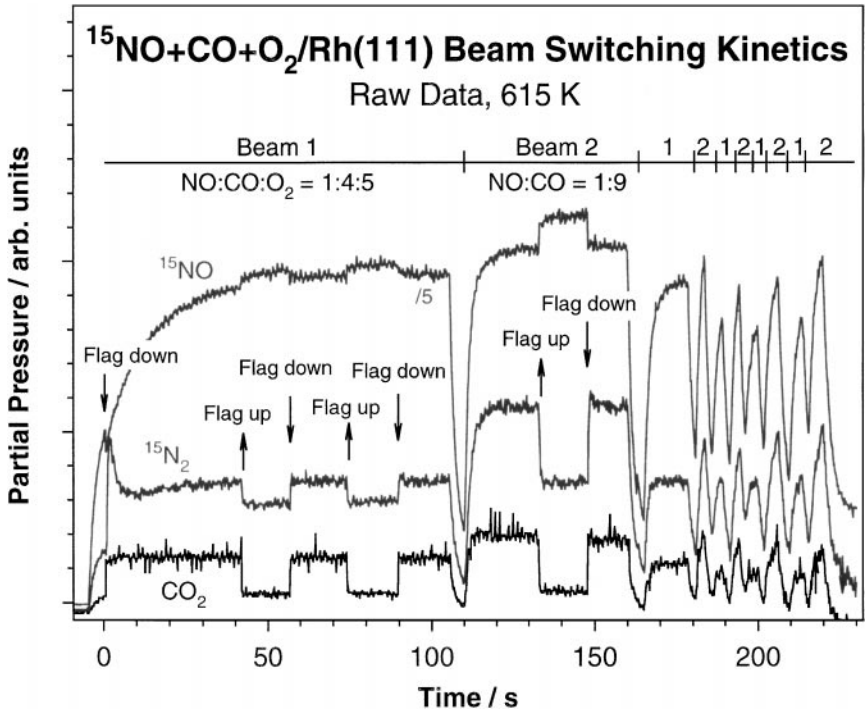

FIG. 11. Typical example of the raw data obtained in beam switching experiments. In this example, the traces for CO_2, $^{15}N_2$, and ^{15}NO are shown as a function of time as the composition of the beam is switched between 1 : 4 : 5 (oxygen-rich) and 1 : 9 : 0 (oxygen-lean) $^{15}NO : CO : O_2$ compositions. The temperature of the Rh(111) surface was kept constant at 615 K throughout the whole experiment. Clearly, the rates for both CO_2 and N_2 production are higher with the CO-rich beam in this case, but the changes in reactivity seen here are completely reversible. Also important to notice are the transient kinetics sometimes observed right after beam switching (this is the most noticeable here for $t = 0$–10 s).

beam displays an initial nitrogen production rate one third that seen after switching to the 1 : 9 : 0 gas mixture, and that the rate of CO_2 production also increases with the CO-rich beam, although not as much. The NO uptake is higher in the absence of oxygen, and no detectable O_2 is consumed at any stage of the experiments. Fast switching clearly indicates that the NO reduction efficiency of the rhodium surface deteriorates under net oxidizing conditions, apparently because of the inhibiting effect that O_2 exerts on the NO and/or CO adsorption. It is also clear from the data in Fig. 11 that the changes induced by changing the beam composition are completely reversible: the original steady-state reactivity of the catalyst is easily regained by restoring the same beam composition.

Similar beam switching experiments were also carried out with $CO + O_2$ mixtures (results not shown). Like with the $NO + CO + O_2$ beams, the oxygen-rich beam in this case displays lower steady-state oxidation rates than with the oxygen-lean composition. On the other hand, a clear uptake is seen for oxygen in the steady-state regime during the exposure of the surface to the oxygen lean (7 : 1) beam. Oxygen consumption was measurable with the $CO + O_2$ beams but not with the corresponding $NO + CO + O_2$ gas mixtures.

4. DISCUSSION

The steady-state kinetic data reported here focus on the characterization of the effect that oxygen has on the reduction of NO by CO on Rh(111) surfaces. It could be thought that the addition of oxygen is detrimental to the conversion of $NO + CO$ mixtures, because oxygen is expected to consume some of the carbon monoxide required to reduce the nitrogen oxide. Typically, O_2 is likely to compete with NO for the CO in the mixture. However, there are also other more subtle effects that need to be considered to understand the reactivity of the $NO + CO + O_2$ ternary mixture. In particular, the deposition of oxygen can alter the adsorption properties of the rhodium surfaces. As an extreme of this, subsurface oxygen is known to change the nature of the metal at temperatures above 600 K (66). Another related issue pertinent to the kinetics of this system is the change in adsorption dynamics due to a competition among NO, CO, and O_2 molecules for adsorption sites. Oxygen may inhibit the sticking of the other reactants, but may also remove excess CO in some circumstances, helping, not poisoning, the overall NO reduction reaction. In the following paragraphs, the results from our kinetic studies of the $NO + CO + O_2$/Rh(111) system are analyzed in terms of these ideas.

4.1. *Effect of O_2 on the NO + CO Kinetics*

The kinetic data for the reaction between NO, CO, and O_2 on Rh(111) surfaces presented here strongly suggest that the mechanism for NO reduction in this mixture does not differ much from that operative in the absence of O_2 (12). In particular, the transients seen in the kinetic raw data upon blocking and unblocking of the beam with $NO + CO + O_2$ beam mixtures corroborate the fact that the rate-limiting step in the steady-state NO conversion reaction at intermediate temperatures still appears to be the production of N_2 molecules (Figs. 1 and 3). Notice in particular the contrast between the immediate response of the rate of CO_2 production to the flag removal in the steady state of the kinetic runs at all temperatures and beam compositions, and the slow approach of the N_2 production traces to their steady-state levels below 600 K. The data in Figs. 1 and 3 also provide evidence for the need of the presence of a critical nitrogen coverage on the surface to sustain the catalytic conversion of NO to N_2 at low temperatures (13, 14).

On the other hand, the addition of O_2 to $NO + CO$ mixtures typically lowers the rate of N_2 production (Fig. 5). This effect is more visible at high ($\geq$550 K) temperatures. It could be thought that the poisoning by oxygen may be due to it consuming some of the CO in the $NO + CO + O_2$ mixture, that is, to a competition between $CO + NO$ and $CO + O_2$ reactions. However, the rate for $CO + NO$ conversion in the experiments reported here is always faster than that of $CO + O_2$. This is best shown by the $R_{CO_2} - 2R_{N_2}$ data in Fig. 8, which correspond to the carbon dioxide produced by the second reaction. The first thing to notice there is the fact that the difference is never large, and certainly does not represent the fraction of the total CO_2 production expected on the basis of stoichiometric grounds. As an example to better illustrate this point, it may be instructive to compare the different rates for the case where the extra carbon dioxide production is maximum, that is, for a 1 : 10 : 5 $NO : CO : O_2$ beam at 555 K. The rates for CO_2 and N_2 production in that case amount to 0.0446 and 0.0088 ML/s, respectively. That means that every second 0.0175 CO_2 ML is produced via NO conversion while 0.0271 CO_2 ML originates from CO oxidation with the added O_2. This represents a ratio of approximately 1 : 1.55, much higher than the 1 : 10 ratio expected from this mixture if both reactions occur at the same rate. In other words, the rate of NO reduction in this mixture is more than 6 times faster than that of O_2. And the case worked out above is that where the largest $CO_2 - 2 \times N_2$ rate differential was observed; more significant deviations from the stoichiometry ratios are observed in other cases. On the basis of such calculations, it can be concluded that the poisoning effect of oxygen during the reduction of NO by CO on rhodium is not likely to be dominated by the consumption of CO by the added O_2.

A clue to the explanation of the inhibiting effect of molecular oxygen in the production of N_2 from NO comes from the fact that the addition of O_2 to $NO : CO$ beams poisons the production of CO_2 as well (Figs. 3 to 5). Clearly, the

decrease in N_2 formation is not compensated by reactions between CO and O_2, since a significant reduction in the overall consumption of CO is seen instead. At this point we can only speculate on why this is. It is tempting to propose that O_2 inhibits the chemisorption of carbon monoxide on rhodium surfaces, perhaps because of the build-up of some adsorbed atomic oxygen. Alternatively, O_2 may alter the sticking probability of CO in this system. Noticeable changes in sticking coefficients with gas composition have indeed been observed by us previously for the case of NO + CO mixtures (14).

4.2. *Kinetic Synergies in NO + CO + O_2 Gas Mixtures*

There is a synergy between the concentration of oxygen in the gas beam and the temperature at which the N_2 and CO_2 production reaction rates reach their maxima. Specifically, higher O_2 content leads to lower T_{max}. On inspection of the data in Figs. 4 and 5, it becomes clear that this is mostly due to the fact that oxygen poisoning is more acute at high temperatures. The changes in reaction rate with oxygen addition are less pronounced below 550 K, especially in the case of CO_2 production, where no significant rate changes with O_2 addition are observed. The more noticeable character of the oxygen-induced NO reduction inhibition at high temperatures can be easily understood upon inspection of Fig. 9, where it is shown that CO oxidation by O_2 is significant only at low (<600 K) temperatures (12). Provided that NO reduction poisoning is likely to occur via the deposition of atomic oxygen on the surface, removal of those surface species by carbon monoxide is efficient only at low temperatures.

As mentioned above, addition of oxygen to the reaction mixture generally leads to an expected inhibition in the NO reducing activity of the catalyst. On the other hand, addition of CO most often cause the opposite effect (Fig. 6). This is understandable, giving the fact that carbon monoxide is the only reducing agent in the NO + CO + O_2 mixture. Interestingly, similar rate enhancements are seen in the production of both N_2 and CO_2, especially at intermediate temperatures. This argues for a mechanism where the main role of CO is to remove surface oxygen from the surface. That oxygen may originate from dissociation of either NO or O_2, and may poison any subsequent steps if not removed via recombination with CO.

The enhancing effect of CO in the conversion of both NO and O_2 is more noticeable at high temperatures. There is in fact an interdependence between the content of CO in the beam and the reaction temperature: more CO is required to reach the same CO_2 production rates at higher temperatures. The optimum reactivity for N_2 production is seen around 500–600 K, but steady increases in rates with increasing CO gas concentrations are also seen at higher temperatures. This indicates that what controls the recombination of CO with atomic oxygen is its steady-state coverage on the surface. An increase in surface temperature leads to an increase in the CO desorption rate, and therefore an increase in CO flux to the surface is required to maintain comparable CO surface coverages. The fact that the efficiency of CO for removing surface oxygen decreases with increasing temperature was previously observed directly in molecular beam experiments with CO + O_2 mixtures (12).

At the other extreme, low temperatures and high CO concentrations in the gas mixtures can lead to poisoning of the N_2- and CO_2-producing reactions. Notice in particular the drop in activity seen in Fig. 6 at 505 and 555 K for CO : O_2 ratios above approximately 1.5. In this case, the most likely scenario is that the surface becomes poisoned by an excess of chemisorbed carbon monoxide. In fact, almost linear drops in activity are seen with increasing CO content in CO-rich mixtures ($y \geq 10$ in the $1 : y : 5$ NO : CO : O_2 beams) for both N_2 and CO_2 production, suggesting that the CO surface coverage increases linearly with CO partial pressure in that regime. This effect diminishes with temperature, and disappears by 600 K because of the exponential increase in CO desorption rate with T.

Because of the low-temperature CO poisoning of the NO reduction reaction seen with CO-rich beams, an interesting effect can be observed during the addition of oxygen to those mixtures. Indeed, oxygen addition leads to an enhancement, not a reduction, in catalyst activity under such conditions. This observation is perhaps best illustrated by the data in Fig. 7. It is seen there that the rates of N_2 and CO_2 production both increase with increasing O_2 content in the beam at 505 K, until reaching a maximum with a O_2 : CO ratio about 0.5. Again, the initial addition of O_2 to the fuel-rich 1 : 9 NO : CO mixture helps in the removal of excess CO on the surface, facilitating the adsorption and decomposition of NO. An excess of O_2, on the other hand, slows the reaction, because surface CO is replaced by surface oxygen.

Optimum rates are obtained at 505 K with the 1 : 6 : 3 NO : CO : O_2 mixture, but those maxima shift to lower O_2 : CO ratios with increasing temperature. At 555 K, the best mixture for CO_2 formation in Fig. 7 is that with 1 : 7 : 2 NO : CO : O_2 composition, and by 615 K, mixtures with no oxygen are preferred. As the rate of CO desorption increases, less oxygen is needed to keep the surface free of excess CO. Notice, however, that there are subtle differences in behavior between the rates of CO_2 and N_2 production: the formation of N_2 is a bit more sensitive to oxygen addition, so no O_2 is needed in the beam by 555 K. Nevertheless, it can be concluded that the best combinations of beam composition and reaction temperature to optimize both reaction rates are those that lead to stoichiometric surface coverages, the same as in the case of NO + CO mixtures (12, 14). Additional examples of this are given in Fig. 10.

4.3. Effect of NO on the CO + O_2 Conversion

So far we have focused our discussion on the effect that oxygen exerts on the kinetics of NO reduction by CO. It is interesting to point out that, conversely, NO also affects the kinetics of oxidation of CO by O_2. To better understand this effect, a comparison between the data in Figs. 8 and 9 is warranted: Fig. 9 displays the rates for CO_2 production observed with $y-1:z=9-y$ CO : O_2 mixtures, while Fig. 8c summarizes the component of the CO_2 rates observed with $1:y:z=9-y$ NO : CO : O_2 beams corresponding to the CO + O_2 reaction. In most cases, but more dramatically below 600 K, the addition of NO inhibits the consumption of O_2. For instance, for CO : O_2 = 5 : 3 and $T=505$ K, $R_{CO_2}=0.071$ ML/s, but with a 1 : 6 : 3 NO : CO : O_2 beam the rate of O_2 consumption is only 0.011 ML/s (and the total rate of CO_2 production is only 0.039 ML/s). It is clear that NO competes favorably against O_2 for the adsorbed CO, and that the CO + O_2 conversion rate seen in the ternary mixture resembles that of a CO + O_2 beam richer in the second component.

The magnitude of the inhibition of the CO + O_2 reaction with NO addition diminishes as the CO : O_2 ratio is varied away (in either direction) from stoichiometry, and also as the temperature of the surface is increased. Once again, a synergy is seen here: the reduction in rate maxima for CO + O_2 with NO addition shifts to higher temperatures with increasing amounts of CO in the beam. As discussed before, the interconnection between temperature and beam composition is directly related to the steady-state coverage of carbon monoxide on the Rh(111) surface. Notice, however, that NO addition not only inhibits the consumption of molecular oxygen, but in fact reduces the total amount of CO_2 produced. It appears that CO adsorption is restricted in that case as well. It is worth remembering that NO competes favorably with CO for adsorption sites, diminishing the apparent sticking coefficient of the latter, to the extreme of sometimes displacing adsorbed CO into the gas phase (14).

The reduction in oxygen consumption with NO diminishes considerably at higher temperatures, and becomes negligible above 600 K for CO : O_2 ratios above 10 : 1 or below 1 : 1. Recall that under those conditions N_2 production is low too, and that the overall activity of the catalyst is dominated by the CO + O_2 reaction. Under those circumstances, the surface is most likely covered with some oxygen. Our earlier studies on the adsorption of NO on clean Rh surfaces (11) have shown that the initial sticking coefficient in that case is constant up to 800 K. On the other hand, that sticking coefficient is affected by the presence of other gases in the beam mixture (14), and appears to decrease rapidly as the oxygen coverage increases on the Rh surface. It is also well established that the extent of NO dissociation decreases with oxygen coverage (25, 48).

4.4. Hysteresis Effect on the NO + CO + O_2 Reaction

Two more points are worth discussing briefly here. The first is the hysteresis in steady-state reaction rates seen in Fig. 2 as the temperature of the crystal is ramped upward and downward. The data in that figure demonstrate that there are some basic differences in behavior between the reactions carried out while heating an initially clean surface and those carried out while cooling or subsequently heating the sample. In more general terms, this suggests that the reactivity of the catalyst may depend on the history of the process. However, it is interesting to note that nitrogen production is not affected seriously by these changes; only the production of CO_2 is. We believe that there could be more than one reason for the hysteresis reported in this paper. Those include (1) the formation of subsurface oxygen above 600 K; (2) the formation of nitrogen surface islands at low temperatures and moderate oxygen coverage; and (3) surface structural modifications.

At the beginning of the NO + CO + O_2 reaction from a clean metal at low temperatures, a fast build-up of nitrogen surface islands takes place, while the oxygen coverage remains low. Our previous isotopic-labeling studies on the NO + CO/Rh(111) system have shown that below 600 K a critical atomic nitrogen coverage needs to build up on the surface before the system reaches its steady-state behavior (12–14). As the temperature of the surface is increased, however, the overall nitrogen coverage decreases rapidly, while that of oxygen increases. It is possible that when cooling the crystal from high temperatures, at least some of the oxygen deposited may remain on the surface, altering its catalytic behavior. In particular, it is quite likely that oxygen atom incorporation into the subsurface is irreversible, and that those species remain in the solid upon cooling of the sample. Oxide formation has been reported to alter the adsorption and catalytic properties of rhodium (21, 67).

In addition to the explanation provided above, the difference in behavior of the rhodium surface with different pretreatments may be also due, at least in part, to dynamic changes during the exposure of the crystal to the molecular beams. Recall the variations in surface coverages apparent from the raw data in Figs. 1 and 3 when heating from 505 to 555 K and from 555 to 615 K. Specifically, the production of carbon dioxide does not immediately adjust to the change in temperature in that temperature range, but rather displays an induction period a few seconds long. On the other hand, a significant amount of nitrogen desorption is clearly seen in the same time interval as a spike in the partial pressure traces; CO_2 production increases once the excess surface nitrogen is eliminated. In the other direction, clear but small increases in CO_2 production are seen during cooling 555 to 505 K, while no change in nitrogen production is observed there (data not shown). Finally, in experiments where the kinetic cycle is started at high temperatures by cooling of the surface, the reaction maxima for N_2 production shift

to lower temperatures (from 555 to 505 K in the example cited in the Results section), while those for CO_2 do not change.

These results point to a complex interplay among the coverages of the different adsorbed species. On one hand, it has already been established that at low temperatures nitrogen islands form on the surface (12–14). On the other hand, nitrogen is replaced by oxygen at higher temperatures. The deposition of strongly bonded N atoms at low temperatures is likely to be reversible, but the deposition of oxygen may not be. Also, oxygen coadsorption does affect the adsorption of nitrogen (11, 32, 39, 44), and may very well change the nature of the nitrogen islands required to maintain the steady-state catalytic behavior. Complex changes were reported previously on the surface upon nitrogen and/or oxygen build-up on Rh(111) in scanning tunneling microscopy experiments (52). Finally, a similar behavior observed by Comelli and co-workers on Rh(110) was attributed to surface structural modifications (46, 48). All nitrogen islands, surface and subsurface oxygen, and surface reconstruction may play a role in the reaction hysteresis reported here.

4.5. *Fuel-Lean/Fuel-Rich Cyclic Processes*

The ultimate goal of the present work is to suggest a better way to manage NO reduction under the conditions encountered in real automobile exhausts. One important new development in the technology of three-way catalysts is the need to improve their NO removal performance under net oxidizing conditions, because that would lead to better fuel efficiency (1, 2). Vehicle manufacturers are considering an option where engines are operated under lean air-to-fuel (A/F) ratios (with excess air) during cruising, and returned to stoichiometric operation when more power is required (68).

From this point of view, it is interesting to investigate the behavior of the catalyst while oscillating the beam composition between oxygen-rich and fuel-rich conditions. This idea was briefly explored here; an example of the results from that work is shown in Fig. 11. On the basis of what was learned from the kinetic studies reported above, rhodium surfaces are expected to become covered with atomic oxygen during their exposure to oxygen-rich beams. This reduces the overall reducing activity of the catalyst. Under CO-rich conditions, on the other hand, nitrogen and/or CO are the dominant species on the surface, and higher nitrogen production rates can be achieved. What is interesting from the data shown in Fig. 11 is the fact that these changes appear to be reversible, at least at temperatures of 615 K or below. This means that the activity of the catalysts, once poisoned by oxygen under oxygen-rich conditions, can be recouped via exposure to fuel-rich mixtures. It appears that surface-reducing agents (CO in the present case, volatile organic compounds in most practical engines) can effectively remove the surface oxygen as CO_2. On the other hand, it was also seen that excess CO reduces the activity of the catalyst, and should be avoided. Hence, the duration of the fuel-rich pulses used to reduce the catalyst becomes critical.

To better understand how beam alternation can be used to explore cyclic processes, let us expand on the interpretation of the data in Fig. 11. Note, for instance, that the transient in the first few seconds ($t < 5$ s) of Fig. 11 displays a particularly large rate for NO reduction and N_2 production. Similar transient processes are possible when starting with CO-rich beams. Previous transient kinetic studies of the $NO + CO$ reaction have also shown that the NO reduction rates are high when clean Rh surfaces are exposed to $NO + CO$ beams at high temperatures, but that they decrease drastically as the reaction approaches its steady state (14). The time required to approach this steady state decreases with increasing temperature or increasing NO : CO ratio. This points to the design of rapid cycles with relative short fuel-rich pulses. During exposure to oxygen-rich mixtures, the rhodium surface becomes increasingly covered by oxygen, and that helps to lower the nitrogen coverage (because of strong repulsive forces between N and O atoms). If the oxygen-rich regime were to be kept short, higher NO reducing activity would be obtained, because NO molecules decompose preferentially during the transient even in the excess of gas-phase O_2. When the composition of the gas is switched to a fuel-rich composition, the surface oxygen is removed via CO_2 formation, enhancing the activity of the catalyst toward NO reduction. The critical point to be remembered here is that while the CO_2 formation and its desorption are instantaneous, N_2 desorption requires some time to reach its steady-state level. By never allowing the NO reduction reaction to reach its steady state, it may be possible to take advantage of the high rates sometimes seen in the transient regimes. The kinetic optimization of cyclic NO conversion processes is worth further research.

4.6. *Comparison with Previous Results*

The new ideas on the $NO + CO + O_2$/Rh(111) system developed in this study should be added to the extensive work reported in the past, in particular that carried out at the General Motors (GM) laboratory. In terms of the conversion of $CO + O_2$ mixtures under ultrahigh vacuum, Schwartz *et al*. found that the dependence of the rate law on CO partial pressure goes from negative for CO-rich mixtures to positive under oxidizing conditions (69). Also, the surface was found to be primarily covered with CO below 400 K, while oxygen was the dominant surface species between 425 and 900 K. All this supports our hypothesis that CO poisoning at low temperatures is gradually replaced by oxygen inhibition as the temperature of the surface is increased. Moreover, oxygen poisoning via rhodium oxide formation was inferred from experiments under atmospheric conditions (27, 39). Interestingly, the authors found in that study that under steady-state reaction conditions the

surface is covered largely with adsorbed N atoms together with smaller amounts of adsorbed NO. More recently, Belton and co-workers concluded from kinetic and infrared experiments carried out on Rh(111) with $NO + CO + O_2$ mixtures at high pressures that oxygen does not seem to affect the $NO + CO$ reaction kinetics, and that O_2 consumption is adsorption-rate limited, with the NO–CO adsorption–desorption equilibrium controlling the vacant sites required for the dissociation of that molecule (38).

Although the agreement between the GM work (particularly the recent work of Permana *et al.*) and ours is excellent, a number of differences can be identified. To begin with, no N_2O was ever produced in the reactions reported in the present paper, even though N_2O amounts comparable to or larger than those seen for N_2 were reported at high pressures below 700 K (38). Also, higher selectivity toward N_2 was observed above 600 K at low P_{NO} (≤ 0.8 Torr), but the yield for the NO reduction to N_2 was below 15% under those conditions. We explain this discrepancy by the changes in selectivity expected with varying gas pressures because of the concomitant changes in surface coverages. We have reported recently, based on steady-state kinetic measurements with isotopic labeling switching, that N_2 production under the conditions of the catalytic reaction is likely to involve the formation of a N–NO species (15). This intermediate is presumed to be common for the production of both N_2 and N_2O, so the selectivity between the two pathways must be dominated by the relative probabilities for N–NO decomposition (to N_2 + adsorbed O) versus molecular desorption. Higher reactant pressures are likely to result in higher surface coverages, and in the blocking of the empty sites required for N_2O surface dissociation. This argument may explain why the selectivity toward N_2 formation is reduced with increasing reaction pressures, but needs to be tested directly with experiments at intermediate pressures.

A second point of disagreement between the previous reports and our work is in the proposal of the rate-limiting step for the reduction of NO and the formation of N_2. The GM group proposes dissociation of adsorbed NO as rate-limiting (38). We, on the other hand, believe that the overall kinetics is controlled by the production of N_2, which, as mentioned earlier, appears to occur via N–NO formation. The main supporting evidence for our claim comes from the slow response of the N_2 partial pressure trace to the blocking and unblocking of the beam seen below 600 K (Figs. 1 and 3), the same as with $NO + CO$ mixtures (12, 14). Fast NO dissociation was shown directly by Niemantsverdriet and co-workers by using XPS and SIMS experiments (42, 70). Finally, it is also worth mentioning that the high-pressure experiments display different dependencies on gas composition than our beam studies, in particular in terms of the relative changes between CO_2 and N_2 production rates. For instance, when mixtures with constant $P_{CO} = 4$ Torr and $P_{NO} = 0.8$ Torr are used, an increase in CO_2 production of about an order of magnitude is seen when P_{O_2} is varied from 0.8 to 7 Torr (38). The production of N_2, on the other hand, remains the same throughout the whole O_2 pressure range, and N_2O production declines at $P_{O_2} \geq 3$ Torr. No comparable selectivity changes were seen in our experiments. All three points clearly indicate that the reaction mechanism at high pressures is somewhat different than that under ultrahigh vacuum conditions, at least as far as the relative rates of the different steps are concerned. Again, studies in the intermediate pressure range are warranted.

One of the most important observations from the results presented in this paper is that there is a build-up of a critical coverage of nitrogen atoms on the Rh surface before N_2 desorption can be seen, as in the case of $NO + CO$ reaction (12–15). The fast responses of the NO, CO, and CO_2 partial pressure traces to changes in the beam flux under steady-state conditions unequivocally demonstrate that both NO dissociation and CO_2 formation are faster than N_2 production under most relevant reaction conditions. Furthermore, it was established that oxygen consumption is adsorption-rate limited, since the adsorption of CO and NO appears to control the concentration of the surface vacant sites necessary for dissociative adsorption of oxygen below 600 K. On the other hand, the scenario changes above 600 K, and oxygen removal becomes the slow step. Most of these points could not be brought out by the earlier studies because of the lack of direct evidence on the kinetics of the individual reaction steps. Although our experiments were performed under vacuum, they are likely to reproduce many of the features of the processes that occur under the more realistic catalytic converter conditions once the effect of increasing pressures is properly included.

5. CONCLUSIONS

This paper reports results from a kinetic study on the reaction of $NO + CO + O_2$ mixtures over Rh(111) single-crystal surfaces by using collimated effusive molecular beams. Three different sets of beam compositions were used, namely, $1:9:z$, $1:y:5$, and $1:y:z = 9-y$ $NO:CO:O_2$ ratios, in order to explore the role of adding oxygen and CO to the gas mixture and the changes induced when going from fuel-rich to fuel-lean conditions. Isothermal steady-state kinetic measurements were performed with all three-beam sets for reaction temperatures between 435 and 765 K. These experiments were carried out in ultrahigh vacuum, but under conditions where the NO reduction reaction could be sustained in a catalytic regime similar to that encountered in realistic catalytic converters.

Analysis of the kinetic data led to the conclusion that the main effect of the addition of oxygen to the $NO + CO$ reaction mixture is to inhibit the reaction rates for the production of both N_2 and CO_2 under most circumstances.

This effect is more pronounced at high temperatures, above 600 K, and for the production of nitrogen, which can be completely suppressed by the added O_2 above 700 K. This behavior was explained by the poisoning of surface sites that results from the dissociative adsorption of gas-phase oxygen. Independent kinetic measurements for the reaction between CO and O_2 corroborate this hypothesis. On the other hand, it became clear that the inhibiting effect of O_2 is not due to competition with NO for the CO on the surface, since significant rate reductions are seen for both N_2 and CO_2 reactions. Moreover, the production of CO_2 is appreciably faster with gas $CO + O_2$-only mixtures. The kinetic data clearly point to a preferential reaction of CO with NO instead of O_2; the poisoning caused by the added oxygen in the gas mixture is common to both reactions, and is most likely associated with a reduction in the surface coverage of carbon monoxide.

The addition of excess CO to the reaction mixture also has an inhibiting effect on both N_2 and CO_2 production rates. This effect is, however, only important at low temperatures, below 600 K. In connection with this, it was found that there is an optimum reaction temperature for each given $NO + CO + O_2$ beam composition, and that this optimum temperature increases as the beam becomes richer in CO. This is easily explained by the changes in CO surface coverage induced by increases in surface temperature: higher desorption rates (which increase exponentially with T) lead to lower steady-state CO coverages, and that needs to be compensated by increasing the flux of the CO gas on the surface. At the other extreme, the activity of the surface is poisoned by excess adsorbed CO in experiments with CO-rich beams at low temperatures. Interestingly, the addition of oxygen to the beam in those cases enhances, not poisons, the conversion of NO to N_2, presumably because the added O_2 helps removed any excess CO from the surface.

A hysteresis was observed in the conversion of $NO + CO + O_2$ mixtures during heating and cooling of the surface. This hysteresis can be attributed to a combination of factors, including the formation of subsurface oxygen above 600 K (the most likely cause of the changes), the growth of nitrogen surface islands with different characteristics depending on the history of the catalytic process, and additional surface structural modifications. Finally, beam-alternating methods were tested as a way to manage NO reduction efficiently under net oxidizing conditions. Fast switching between reducing and oxidizing gas mixtures is a promising approach to optimize the performance of automobile engines. The main crux of the beam oscillation concept is that it is possible to take advantage of unique transient kinetic behaviors during NO reduction by performing fast changes in beam composition and not allowing the system to reach steady-state conditions. One of the possibilities to optimize the performance of the catalysts is to maintain the surface relatively free from oxygen poisoning so NO reduction can be carried out under close-to-stoichiometric conditions on the surface despite the variations of the composition of the gas.

ACKNOWLEDGMENTS

This work was supported by a grant from the National Science Foundation (CTS-9812760). Additional funding was provided by CULAR.

REFERENCES

1. Belton, D. N., and Taylor, K. C., *Curr. Opin. Solid State Mater. Sci.* **4**, 97 (1999).
2. Farrauto, R. J., and Heck, R. M., *Catal. Today* **55**, 179 (2000).
3. Wei, J., *Adv. Catal.* **24**, 57 (1975).
4. Hegedus, L. L., and Gumbleton, J. J., *Chemtech* **10**, 630 (1980).
5. Taylor, K. C., "Automobile Catalytic Converters." Springer-Verlag, Berlin, 1984.
6. Taylor, K. C., *Catal. Rev. Sci. Eng.* **35**, 457 (1993).
7. Shelef, M., and Graham, G. W., *Catal. Rev.-Sci. Eng.* **36**, 433 (1994).
8. Obuchi, A., Ohi, A., Nakamura, M., Ogata, A., Mizuno, K., and Ohuchi, H., *Appl. Catal. B* **2**, 71 (1993).
9. Burch, R., and Millington, P. J., *Catal. Today* **26**, 185 (1995).
10. Nakatsuji, T., Yasukawa, R., Tabata, K., Ueda, K., and Niwa, M., *Appl. Catal. B* **21**, 121 (1999).
11. Aryafar, M., and Zaera, F., *J. Catal.* **175**, 316 (1998).
12. Gopinath, C. S., and Zaera, F., *J. Catal.* **186**, 387 (1999).
13. Zaera, F., and Gopinath, C. S., *J. Chem. Phys.* **111**, 8088 (1999).
14. Gopinath, C. S., and Zaera, F., *J. Phys. Chem. B* **104**, 3194 (2000).
15. Zaera, F., and Gopinath, C. S., *Chem. Phys. Lett.* **332**, 209 (2000).
16. Zaera, F., and Gopinath, C. S., *in* "Studies in Surface Science and Catalysis Series," p. 1295. Elsevier, Amsterdam, 2000.
17. Zaera, F., and Gopinath, C. S., *J. Mol. Catal. A* **167**, 23 (2001).
18. Campbell, C. T., and White, J. M., *Appl. Surf. Sci.* **1**, 347 (1978).
19. Dubois, L. H., Hansma, P. K., and Somorjai, G. A., *J. Catal.* **65**, 318 (1980).
20. Becker, W. C., and Bell, A. T., *J. Catal.* **84**, 200 (1983).
21. Oh, S. H., and Carpenter, J. E., *J. Catal.* **80**, 472 (1983).
22. DeLouise, L. A., and Winograd, N., *Surf. Sci.* **159**, 199 (1985).
23. Hendershot, R. E., and Hansen, R. S., *J. Catal.* **98**, 150 (1986).
24. Kao, C.-T., Blackman, G. S., Van Hove, M. A., Somorjai, G. A., and Chan, C.-M., *Surf. Sci.* **224**, 77 (1989).
25. Root, T. W., Schmidt, L. D., and Fisher, G. B., *Surf. Sci.* **134**, 30 (1983).
26. Root, T. W., Schmidt, L. D., and Fisher, G. B., *Surf. Sci.* **150**, 173 (1985).
27. Oh, S. H., Fisher, G. B., Carpenter, J. E., and Goodman, D. W., *J. Catal.* **100**, 360 (1986).
28. Root, T. W., Fisher, G. B., and Schmidt, L. D., *J. Chem. Phys.* **85**, 4679 (1986).
29. Root, T. W., Fisher, G. B., and Schmidt, L. D., *J. Chem. Phys.* **85**, 4687 (1986).
30. Belton, D. N., and Schmieg, S. J., *J. Catal.* **144**, 9 (1993).
31. Belton, D. N., DiMaggio, C. L., and Ng, K. Y. S., *J. Catal.* **144**, 273 (1993).
32. Belton, D. N., DiMaggio, C. L., Schmieg, S. J., and Ng, K. Y. S., *J. Catal.* **157**, 559 (1995).
33. Kim, Y. J., Thevuthasan, S., Herman, G. S., Peden, C. H. F., Chambers, S. A., Belton, D. N., and Permana, H., *Surf. Sci.* **359**, 269 (1996).
34. Peden, C. H. F., Belton, D. N., and Schmieg, S. J., *J. Catal.* **155**, 204 (1995).
35. Permana, H., Ng, K. Y. S., Peden, C. H. F., Schmieg, S. J., Lambert, D. K., and Belton, D. N., *J. Catal.* **164**, 194 (1996).
36. Permana, H., Ng, K. Y. S., Peden, C. H. F., Schmieg, S. J., and Belton, D. N., *J. Phys. Chem.* **99**, 16344 (1995).

37. Herman, G. S., Peden, C. H. F., Schmieg, S. J., and Belton, D. N., *Catal. Lett.* **62**, 131 (1999).
38. Permana, H., Ng, K. Y. S., Peden, C. H. F., Schmieg, S. J., Lambert, D. K., and Belton, D. N., *Catal. Lett.* **47**, 5 (1997).
39. Peden, C. H. F., Goodman, D. W., Blair, D. S., Berlowitz, P. J., Fisher, G. B., and Oh, S. H., *J. Phys. Chem.* **92**, 1563 (1988).
40. Schwartz, S. B., Fisher, G. B., and Schmidt, L. D., *J. Phys. Chem.* **92**, 389 (1988).
41. Ng, K. Y. S., Belton, D. N., Schmieg, S. J., and Fisher, G. B., *J. Catal.* **146**, 394 (1994).
42. Borg, H. J., Reijerse, J. F. C.-J. M., van Santen, R. A., and Niemantsverdriet, J. W., *J. Chem. Phys.* **101**, 10052 (1994).
43. Hopstaken, M. J. P., van Gennip, W. J. H., and Niemantsverdriet, J. W., *Surf. Sci.* **435**, 69 (1999).
44. Hopstaken, M. J. P., and Niemantsverdriet, J. W., *J. Phys. Chem. B* **104**, 3058 (2000).
45. Siokou, A., vanHardeveld, R. M., and Niemantsverdriet, J. W., *Surf. Sci.* **404**, 110 (1998).
46. Baraldi, A., Dhanak, V. R., Comelli, G., Kiskinova, M., and Rosei, R., *Appl. Surf. Sci.* **68**, 395 (1993).
47. Cobden, P. D., Nieuwenhuys, B. E., Esch, F., Baraldi, A., Comelli, G., Lizzit, S., and Kiskinova, M., *Surf. Sci.* **416**, 264 (1998).
48. Comelli, G., Dhanak, V. R., Kiskinova, M., Prince, K. C., and Rosei, R., *Surf. Sci. Rep.* **32**, 165 (1998).
49. Cho, B. K., Shanks, B. H., and Bailey, J. E., *J. Catal.* **115**, 486 (1989).
50. Cho, B. K., *J. Catal.* **148**, 697 (1994).
51. Bugyi, L., and Solymosi, F., *Surf. Sci.* **258**, 55 (1991).
52. Xu, H., and Ng, K. Y. S., *Surf. Sci.* **365**, 779 (1996).
53. Zhdanov, V. P., and Kasemo, B., *Surf. Sci. Rep.* **29**, 31 (1997).
54. van Hardeveld, R. M., Schmidt, A. J. G. W., and Niemantsverdriet, J. W., *Catal. Lett.* **41**, 125 (1996).
55. Makeev, A. G., Janssens, N. M. H., Cobden, P. D., Slinko, M. M., and Nieuwenhuys, B. E., *J. Chem. Phys.* **107**, 965 (1997).
56. Hecker, W. C., and Bell, A. T., *J. Catal.* **88**, 289 (1984).
57. Bowker, M., Guo, Q., Li, Y., and Joyner, R. W., *J. Chem. Soc., Faraday Trans.* **91**, 3663 (1995).
58. Gopinath, C. S., and Zaera, F., in preparation (2001).
59. Liu, J., Xu, M., Nordmeyer, T., and Zaera, F., *J. Phys. Chem.* **99**, 6167 (1995).
60. Zaera, F., Liu, J., and Xu, M., *J. Chem. Phys.* **106**, 4204 (1997).
61. Guevremont, J. M., Sheldon, S., and Zaera, F., *Rev. Sci. Instrum.* **71**, 3869 (2000).
62. "Vacuum Physics and Technology" (G. L. Weissler, and R. W. Carlson, Eds.). Academic Press, New York, 1979.
63. Liu, J., Xu, M., and Zaera, F., *Catal. Lett.* **37**, 9 (1996).
64. Xu, M., Liu, J., and Zaera, F., *J. Chem. Phys.* **104**, 8825 (1996).
65. Öfner, H., and Zaera, F., *J. Phys. Chem.* **101**, 396 (1997).
66. van Hardeveld, M., Ph.D. Thesis, Technische Universiteit Eindhoven, 1997.
67. Castner, D. G., and Somorjai, G. A., *Appl. Surf. Sci.* **6**, 29 (1980).
68. Boegner, W., Kraemer, M., Krutzsch, B., Pischinger, S., Voigtlaender, D., Wenninger, G., Wirbeleit, F., Brogan, M. S., Brisley, R. J., *et al.*, *Appl. Catal. B* **7**, 153 (1995).
69. Schwartz, S. B., Schmidt, L. D., and Fisher, G. B., *J. Phys. Chem.* **90**, 6194 (1986).
70. van Hardeveld, R. M., Borg, H. J., and Niemantsverdriet, J. W., *J. Mol. Catal. A* **131**, 199 (1998).